

Spectroscopic investigation of the generation of "isomerization" states: Eigenvector analysis of the bend-CP stretch polyad

著者	三上 直彦
journal or publication title	Journal of chemical physics
volume	109
number	2
page range	492-503
year	1998
URL	http://hdl.handle.net/10097/35705

doi: 10.1063/1.476586

Spectroscopic investigation of the generation of "isomerization" states: Eigenvector analysis of the bend-CP stretch polyad

Haruki Ishikawa,^{a)} Chioko Nagao, and Naohiko Mikami

Department of Chemistry, Graduate School of Science, Tohoku University, Aoba-ku, Sendai 980-8578, Japan

Robert W. Field

Department of Chemistry, Massachusetts Institute of Technology, Cambridge, Massachusetts 02139

(Received 24 February 1998; accepted 3 April 1998)

The highly excited vibrational levels of HCP exhibit a regular energy level and intensity pattern characteristic of 2:1 bend-CP stretch polyads. Stimulated by the experimental observation of vibrational levels with rotational constants (B -values) 5%–10% larger than other observed levels, Schinke and co-workers noticed that these large- B levels were characterized by atypical nodal structures indicative of large amplitude motion along the minimum energy HCP \leftrightarrow CPH isomerization path [J. Chem. Phys. **107**, 9818 (1997)]. In this paper, we show that the transition from "normal-mode-type" to "isomerization" vibrational states arises naturally out of a traditional spectroscopic (algebraic) effective Hamiltonian polyad model. A global least squares fit, based on this polyad \mathbf{H}^{eff} model, shows that all of the observed "isomerization" states belong to polyads and that the eigenvectors of this \mathbf{H}^{eff} model have the qualitatively distinct nodal structure first noticed by Schinke and co-workers. The "isomerization" states are not indicative of a breakdown of the polyad model; rather they are a natural consequence of this traditional spectroscopic model.

© 1998 American Institute of Physics. [S0021-9606(98)03026-8]

I. INTRODUCTION

In the last two years, experimental and theoretical studies on highly excited vibrational levels of small polyatomic molecules have progressed rapidly.¹ In the high energy region, how to recognize a qualitative change in the character of vibrational levels, such as a transition from a normal- to a local-mode picture or the onset of bond rearrangement in an isomerization reaction, is one of the central issues in this field. In order to elucidate the spectroscopic signature of such dynamics in the high energy region, many theoretical studies have been carried out. These studies include: an analysis of bifurcation/continuation diagrams of the periodic orbits in the classical phase space,² a classification of the phase space sphere,³ and inspection of wave functions obtained by solving the Schrödinger equation using a global potential energy surface (PES).⁴ These are examples of successful methods that document the change in the character of the vibrational modes. In the case of theoretical studies, qualitative changes in structure and dynamics are easily recognized by qualitative changes in the character of wave functions. In the case of the HCN \leftrightarrow CNH isomerization system, for example, Bowman and co-workers calculated vibrational energies and wave functions in the high energy region.⁵ They reported that in addition to the HCN and CNH type states, there appears another type of the vibrational state having a delocalized wave function along the minimum energy

isomerization path from HCN to CNH. One can readily refer to such a vibrational state as a "transition state" of the isomerization.

On the other hand, many spectroscopic techniques, such as dispersed fluorescence (DF), stimulated emission pumping (SEP), and so on, have been developed to obtain information about the highly excited vibrational levels. Since the wave function itself is not an experimental observable, identification of qualitative structure/dynamics changes in a spectrum is less obvious or direct than in a theoretical calculation. In general in spectroscopic studies, the first step is a determination of the molecular constants, such as vibrational energies, rotational constants, and so on, so that the rotation-vibration energies observed can be reproduced by these constants on the basis of a simple spectroscopic (algebraic) Hamiltonian model. The spectroscopic or effective Hamiltonian, \mathbf{H}^{eff} , is based on the harmonic terms and some *specific* anharmonic terms of the potential function. The eigenvalues of \mathbf{H}^{eff} are typically expressed in a Dunham expansion form. In many cases, although the energies and rotational constants of vibrational levels in the high energy region can be reproduced to measurement accuracy by adding higher order anharmonicities and off-diagonal interactions among different vibrational modes, it seems difficult with such a flexible *ad hoc* model to extract any of the qualitative changes in the dynamics or wave functions which are encoded in the spectra.

Recently, both experimental and theoretical investigations on highly excited vibrational levels of the $\tilde{X}^1\Sigma^+$ state of HCP have progressed. Although HCP is a homolog of HCN, the linear CPH configuration corresponds to a saddle point rather than a local minimum of the PES.^{6–8} However,

^{a)} Author to whom correspondence should be addressed. Electronic mail: haruki@qclhp.chem.tohoku.ac.jp

one can consider the HCP \leftrightarrow CPH system as a prototype of isomerization, especially with respect to the profound change in the nature of the HC vs HP chemical bond. In order to investigate highly excited vibrational levels, DF and SEP spectroscopies are very powerful techniques. In principle, DF and SEP spectra provide the same information. However, the former provides a global picture whereas the latter provides more precise information. Thus, the complementary use of both the low resolution DF and high resolution SEP techniques is quite valuable. The first study on the highly excited vibrational levels of HCP was carried out by Lehmann and co-workers on the $\tilde{A}^1A'' \rightarrow \tilde{X}^1\Sigma^+$ DF spectrum.⁶ They observed 94 vibrational levels having vibrational energies, E_{VIB} , up to 16 917 cm^{-1} in the \tilde{X} state. All of the levels observed were assigned as combination levels of the bend and CP-stretch modes. They found a surprisingly harmonic behavior of a series of vibrational levels which they ascribed to overtones of the bending mode. They also fitted the vibrational energies using a rigid bender model and obtained a good fit. Later, in order to elucidate the isomerization of the HCP system, Field and co-workers investigated the highly excited vibrational levels of HCP by SEP spectroscopy.^{9,10} They found abrupt changes of the rotational, B , and vibrational fine structure constants in the vicinity of $v_{\text{bend}}=36$. They claimed that these features are due to a change in the resonance structure of the PES.¹⁰ They also observed $\tilde{C}^1A' \rightarrow \tilde{X}^1\Sigma^+$ SEP spectra which sampled vibrational levels in the 18 300–18 800 and 22 500–23 200 cm^{-1} energy regions. In the former case, bend-CP stretch polyads, $(0,30-2m,m)$ and $(0,38-2m,m)$, were clearly observed. In the latter case, several levels were observed having much larger B -values relative to that of the vibrational ground state. These large- B levels were considered to be members of another bend-CP stretch polyad with $v_{\text{CH}} \neq 0$. They considered that the origin of such large B -values was a $1\omega_{\text{CH}}:3\omega_{\text{bend}}$ Coriolis interaction and that the appearance of this type of resonance was indicative of a qualitative change in the vibrational structure.

An extensive theoretical study on this HCP \leftrightarrow CPH system was carried out by Schinke and co-workers.^{8,11} They analyzed bifurcation/continuation diagrams of classical POs and also obtained quantum mechanically all the vibrational energy levels and wave functions up to $E_{\text{VIB}}=23\,000\text{ cm}^{-1}$ from an *ab initio* PES. They found that two distinct families of bending states exist in the higher energy region. One of these families is associated with vibrational levels where the wave function is confined to range of rather small bending angles, that is, near linear “normal-mode-type” states. On the other hand, the wave functions of the other family, i.e., the large amplitude bending states, are closely related to the isomerization path from H-CP to CP-H. Therefore, the latter type of bending states is referred to as “isomerization” or SN states.^{8,12} Schinke and co-workers assigned the vibrational quantum numbers of each level by the number and locations of the nodes of its wave function. In addition, for each “isomerization” level that appears, a corresponding member of the bend-CP stretch polyad was found to be missing. Although the wave functions of the “isomerization”

levels are much different from those of the “normal-mode-type” ones, Schinke and co-workers formally assigned the “isomerization” levels as members of bend-CP stretch polyads.¹¹ However, it was not clear to Schinke and co-workers whether the “isomerization” levels were generated from the polyads or symptomatic of the breakdown of the polyads.

In order to identify experimentally the “isomerization” states and then to explain how they were generated, we have carried out new DF and SEP experiments on this system. In our previous Communication,¹³ we have briefly reported that the “isomerization” levels were experimentally identified based on the agreement with theoretical predictions of their spectroscopic features, such as large rotational constants, specific onset energy, and strong anharmonicity. Our present objective is to demonstrate whether the “isomerization” states can be generated from the bend-CP stretch polyad structure derived from experimental observations. For this purpose, we have carried out a global least-squares fit of the observed vibrational energies of the polyads on the basis of a traditional spectroscopic Hamiltonian model. We have also examined the eigenvectors obtained as a result of the diagonalization of the zero-order Hamiltonian matrix. This eigenvector analysis provides a very clear interpretation of the nature of the “isomerization” states and how these states are generated by the polyad model. In this paper, we report a detailed description of the new DF and SEP spectra of the highly excited vibrational levels of HCP and an interpretation expressed in terms of the bend-CP polyads.

II. EXPERIMENT

Two dye lasers (Lumonics HD-500) were pumped by the second or third harmonic of the output of a Nd:YAG laser (Continuum Powerlite 9010). One of the outputs of the dye lasers was frequency doubled by a β -BBO crystal and used as the PUMP pulse. Depending on the necessary DUMP transition frequency, the fundamental or frequency doubled output of the other dye laser was used as the DUMP pulse. In order to avoid saturation effects, laser intensities were reduced to 50 and 300 μJ for the PUMP and DUMP pulses, respectively. The time delay between two laser pulses was less than 10 ns. The PUMP laser pulse was divided into two portions by a beamsplitter and then introduced into two identical signal and reference fluorescence cells filled with about 700 mTorr of HCP. The DUMP laser pulse was introduced only to the signal cell. The fluorescence signals from these two cells were differentially amplified, in order to compensate for the fluctuations of the PUMP laser pulse intensity. To record the DF spectra, a 25 cm monochromator (Nikon P250) was used. Typical resolution of the DF spectra was 0.8 nm.

HCP was synthesized by the method described elsewhere.⁹

III. BEND-CP STRETCH POLYAD

The equilibrium structure of the $\tilde{X}^1\Sigma^+$ electronic ground state of HCP is linear. Thus, each vibrational level can be specified by using four quantum numbers as (v_1, v_2^l, v_3) ,

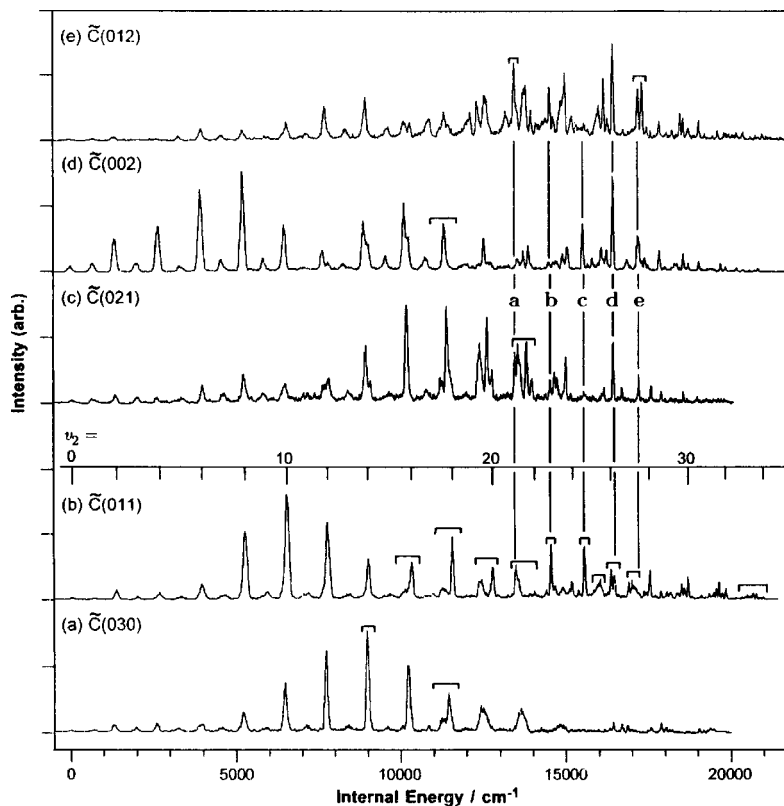


FIG. 1. Dispersed fluorescence spectra of the $\tilde{C}^1A' \rightarrow \tilde{X}^1\Sigma^+$ transition of HCP. The intermediate levels used are indicated on the figure. Vibrational bands that were investigated by SEP spectroscopy are also indicated.

where v_1 , v_2 , v_3 , and l are the quantum numbers for CH stretch, degenerate bend, CP stretch, and vibrational angular momentum, respectively. In the case of HCP, it is well known that there is an anharmonic (Fermi) resonance between the (v_1, v_2^l, v_3) and $(v_1, (v_2 - 2)^l, v_3 + 1)$ levels. Winnewisser and co-workers analyzed this bend-CP stretch resonance and obtained interaction energies between the zero-order (unperturbed) levels, W , to be 11.905 and 16.340 cm^{-1} for the $(0, 2^0, 0) - (0, 0^0, 1)$ and $(0, 3^1, 0) - (0, 1^1, 1)$ pairs, respectively.¹⁴ This anharmonic resonance creates the polyad structure. Here, we define a polyad quantum number, P , as $P = v_2 + 2v_3$. Then, the vibrational levels having the same P and l values interact with each other: $(0, P, 0) \leftrightarrow (0, P - 2, 1) \leftrightarrow (0, P - 4, 2) \leftrightarrow \dots \leftrightarrow (0, 0, P/2)$. When the interactions among the zero-order states in a polyad become sufficiently strong, labeling the vibrational levels by v_2 and v_3 loses its meaning. Thus, hereafter, we will refer to the zero-order basis states as (v_1, v_2, v_3) , while the eigenstates are referred to as $[v_1, P, i]$ where i represents the energy rank in each polyad and runs from 0 (the highest) to $P/2$ (the lowest). For instance, the highest energy member of the polyad with $v_1 = 0$ and $P = m$ is represented as $[0, m, 0]$. This bend-CP stretch polyad is the most fundamental vibrational structure of the HCP system and plays the central role in our investigation of the generation of the “isomerization” levels, as described below.

IV. RESULTS AND DISCUSSION

A. $\tilde{C}^1A' \rightarrow \tilde{X}^1\Sigma^+$ DF and SEP spectra of HCP

Figure 1 shows HCP $\tilde{C}^1A' \rightarrow \tilde{X}^1\Sigma^+$ DF spectra. Inter-

mediate levels used are indicated in the figure. The abscissa represents the internal energy in the electronic ground state. As can be seen, a long even- v_2 progression was clearly recognized in each spectrum. The selection rules for the $\tilde{C}^1A' - \tilde{X}^1\Sigma^+$ transition are $\Delta J = \pm 1$ and $|K'_a - l| = 0$, where K'_a is a projection of the total angular momentum, J , onto the a -axis in the upper state. Since $K'_a = 0$ levels are chosen for the intermediate states, only the $l = 0$ levels, that is, even- v_2 levels, can be observed in this study. Several weak bands, that appeared between the intense bands, can be assigned as “forbidden” transitions to the $l = 1$ levels due to the axis-switching effect. As the internal energy increases, the spectral patterns become more complicated. For instance, Fig. 1(b) shows a DF spectrum whose intermediate is the $\tilde{C}(0, 1, 1)$ level. In a lower energy region, $E_{\text{VIB}} \leq 10\,000 \text{ cm}^{-1}$, each band pattern is very regular. In the middle energy region, $10\,000 \text{ cm}^{-1} \leq E_{\text{VIB}} \leq 14\,000 \text{ cm}^{-1}$, two kinds of bands appear, sharper and broader ones. The sharper DF bands can be assigned as members of a continuation of the regular pattern from the lower energy region. In the higher energy region, $E_{\text{VIB}} \geq 15\,000 \text{ cm}^{-1}$, the band pattern becomes very complicated. However, the even- v_2 progression can still be recognized even in the high energy region. Note that several bands, denoted **a-e**, have relatively large intensities yet they seem not to be members of the even- v_2 progression. In order to obtain more detailed information, we have recorded SEP spectra. The energy regions where SEP spectra were recorded are specified in Fig. 1 for each intermediate state.

Figure 2 shows a typical SEP spectrum observed in this

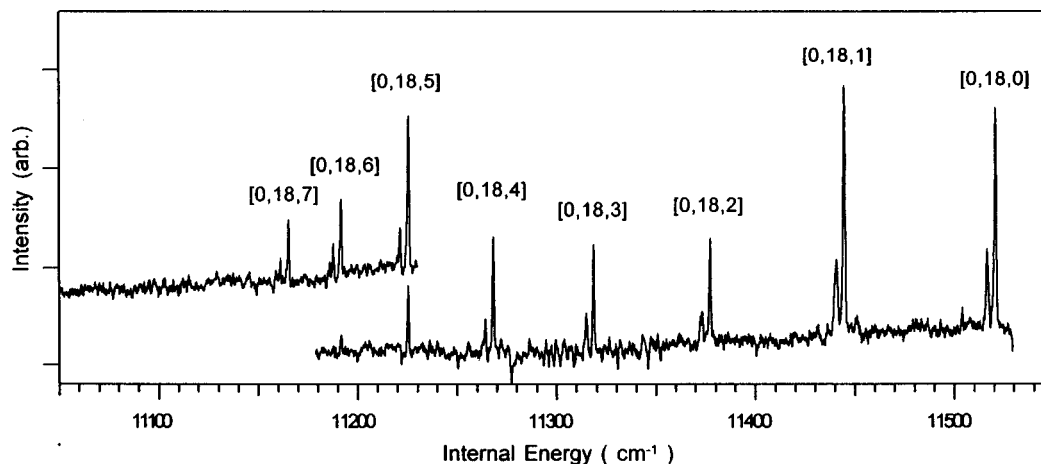


FIG. 2. Stimulated emission pumping spectrum of HCP. The PUMP transition was the $\tilde{C}^1A'(0,3,0) \leftarrow \tilde{X}^1\Sigma^+(0,0,0)$ $P(2)$ line. Vibrational assignments are indicated on the figure.

study. The $\tilde{C}(0,3,0) \leftarrow \tilde{X}(0,0^0,0)$, the $P(2)$ rotational line was used as a PUMP transition. Since the $\tilde{C}^1A' - \tilde{X}^1\Sigma^+$ transition is of parallel type, only P and R rotational lines are allowed. Eight vibronic bands are resolved in the SEP spectrum, whereas they appear as a single broad band in the DF spectrum, Fig. 1(a). All of the vibrational levels sampled in this spectrum are assigned as members of the $P=18$ polyad. We also observed additional SEP spectra which sampled the

same $P=18$ polyad using other intermediate levels. As shown Fig. 3, the Franck-Condon (FC) patterns are different from each other. The broad bands that appeared in the DF spectra as mentioned above are well resolved in the SEP spectra. Moreover, *all* levels that correspond to *both* broad and sharp bands in the DF spectra may be assigned as members of a bend-CP stretch polyad, as described later.

The FC pattern conveys one useful form of information about the wave function. Assuming the case that only one of the zero-order states in each polyad is FC active in the electronic transition, the relative intensity distribution within the polyad should be same for all the spectra recorded via different intermediate levels. This is the case for the $\tilde{A} - \tilde{X}$ transition of acetylene.¹⁵ In that case, a complicated spectrum can be decomposed to each FC bright state component based on the FC pattern. On the contrary, the FC patterns in our SEP spectra of HCP indicate that at least two zero-order levels have nonzero FC intensities and that the observed differences in the relative intensity distribution are due to interference between the FC intensities. Thus, it seems difficult to obtain information about the wave function from the FC patterns alone.

The vibrational term values and rotational constants observed in this study are listed in Table I. Note that the B -values of the levels corresponding to **a-e** are much larger than those obtained from the analysis of the vibrational levels in the lower energy region. Based on the theoretical predictions by Schinke and co-workers, the "isomerization" levels have much larger B -values than that of the $(0,0^0,0)$ level. Since it had been predicted that the onset energy of the "isomerization" levels occurs at $15\,000\text{ cm}^{-1}$, it seemed significant to us that the onset energy of the large- B levels observed in this study is found to be very close to this energy. Thus, we assigned these large- B levels as "isomerization" levels. As will be described below, an eigenvector analysis of the bend-CP stretch polyad also supports this assignment, based on qualitative changes in their wave functions.

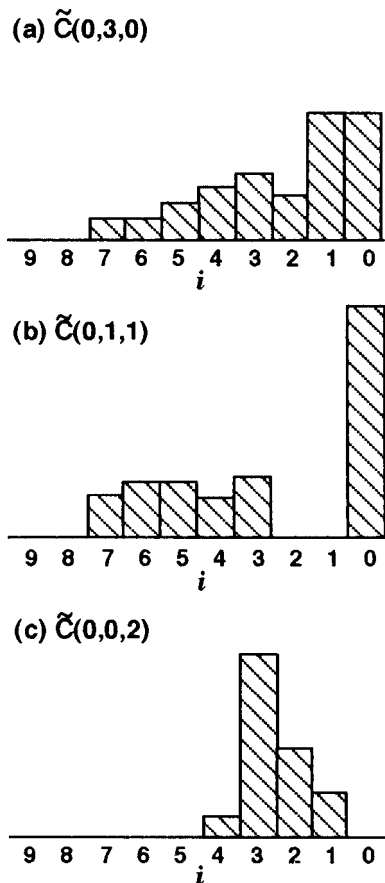


FIG. 3. Relative Franck-Condon intensity patterns of the $\tilde{C}^1A'(0,v_2,v_3) \rightarrow \tilde{X}^1\Sigma^+ P=18$ polyad.

TABLE I. Molecular constants of highly excited vibrational levels of HCP observed in this study.

$[v_1, P, i]$	G_v^a	B_v^b	D_v^b	$J_{\text{obs.}}^c$	$[v_1, P, i]$	G_v^a	B_v^b	D_v^b	$J_{\text{obs.}}^c$
[0,14,0]	9045.05	0.68		set A	[0,26,3]	16063.93	0.66		set A
[0,14,1]	8976.96	0.65		set A	[0,26,4]	15998.77	0.68		set A
					[0,26,5]	15943.52	0.67		set A
[0,16,0]	10286.96	0.659	-25	set B	[0,26,6]	15896.35	0.63		set A
[0,16,1]	10214.69	0.660	-2	set B	[0,26,7]	15858.29	0.65		set A
[0,16,3]	10095.84	0.661	-19	set B	[0,26,8]	15790.35	0.67		set A
[0,16,5]	10010.61	0.661	5	set B					
					[0,28,2]	17298.96	0.652	34	set C
[0,18,0]	11516.74	0.660	3	set B	[0,28,4]	17151.59	0.650	32	set C
[0,18,1]	11440.73	0.660	13	set B	[0,28,5]	17093.35	0.64		set A
[0,18,2]	11373.44	0.662	29	set B	[0,28,6]	17043.93	0.64		set A
[0,18,3]	11314.89	0.652	-32	set B	[0,28,13]	16412.60	0.710	31	set B band d
[0,18,4]	11264.08	0.663	47	set B					
[0,18,5]	11221.40	0.660	22	set B	[0,30,15]	17172.40	0.721	-3	set C band e
[0,18,6]	11187.83	0.654	-17	set B					
[0,18,7]	11161.20	0.664	-28	set B	[0,34,1]	20811.19	0.65		set A
					[0,34,2]	20707.71	0.64		set A
[0,20,0]	12734.71	0.662	30	set B	[0,34,3]	20619.28	0.63		set A
[0,20,1]	12655.05	0.654	-22	set B	[0,34,4]	20532.60	0.67		set A
[0,20,2]	12583.30	0.659	8	set B	[0,34,5]	20470.87	0.65		set A
[0,20,3]	12520.44	0.655	-15	set B					
[0,20,4]	12466.22	0.650	-50	set B	unassigned vibrational levels				
[0,20,5]	12420.18	0.653	-25	set B	13165.17	0.653	27		set C
[0,20,6]	12381.86	0.654	-1	set B	13505.47	0.668	22		set C
[0,20,7]	12355.83	0.654	-19	set B	15505.28	0.700	26		set C band e
[0,20,8]	12311.46	0.679	3	set B	17271.01	0.695	41		set C
[0,22,0]	13942.04	0.67		set A					
[0,22,1]	13857.49	0.64		set A					
[0,22,2]	13781.95	0.66		set A					
[0,22,3]	13715.52	0.66		set A					
[0,22,4]	13657.43	0.65		set A					
[0,22,5]	13607.82	0.65		set A					
[0,22,6]	13566.45	0.66		set A					
[0,22,7]	13534.89	0.68		set A					
[0,22,9]	13426.86	0.690	52	set C band a					
[0,22,10]	13338.77	0.67		set A					
[0,24,10]	14496.60	0.692	23	set C band b					

^aValues of G_v were obtained as the term values of $J=0$ levels when $J=0$ levels were observed. In the case of data set D, the values of G_v were extrapolated using the term values of $J=1$ and 3 levels.

^bIn the case of data sets B and C, the values of B_v and D_v were obtained from the least squares fit using the equation $T = G_v + B_v J(J+1) - D_v [J(J+1)]^2$. Uncertainties for the values of B_v and D_v are 0.017 and 0.000153 cm^{-1} for set B, and 0.011 and 0.000084 cm^{-1} for set C, respectively. In the case of sets A and D, the values of B_v were obtained as $B_v = [T(v, J=2) - T(v, J=0)]/6$ and $B_v = [T(v, J=3) - T(v, J=1)]/10$, respectively.

^cRotational levels observed in each vibrational level were grouped into 4 sets as follows. set A: $J=0,2$, set B: $J=0,2,4,6,8,10$, set C: $J=0-11$, and set D: $J=1,3$.

B. The global fit of all bend-CP stretch polyads

The next concern is how the ‘‘isomerization’’ levels are prepared: are the ‘‘isomerization’’ levels generated by the polyad \mathbf{H}^{eff} or are they produced by a breakdown of the polyad model. In order to investigate this matter, we have started with a global fit of all bend-CP stretch polyads.

The procedure for the global fit of the bend-CP stretch polyad structure of HCP is described here. Due to the bend-CP stretch Fermi resonance, vibrational term values can be reproduced not by a simple Dunham expansion but by a diagonalization of an effective Hamiltonian matrix. In each step of the nonlinear-least squares fit, a diagonalization of the zero-order vibrational Hamiltonian matrix was carried out. In our treatment, interpolyad interactions were ignored, since those would correspond to a higher-order perturbation.

Thus, the Hamiltonian matrix was block-diagonalized for each polyad quantum number, P . The zero-order (unperturbed) vibrational energies, i.e., the diagonal matrix elements, are expressed using a Dunham expansion as

$$\begin{aligned} \langle v_1, v_2^l, v_3 | \mathbf{H}^{\text{eff}} | v_1, v_2^l, v_3 \rangle = & \sum_i \omega_i^0 v_i + \sum_{i \geq j} x_{ij}^0 v_i v_j \\ & + \sum_{i \geq j \geq k} y_{ijk}^0 v_i v_j v_k + g_{22} l^2, \end{aligned} \quad (1)$$

while the off-diagonal matrix elements for each block are¹⁶

TABLE II. Observed and calculated vibrational term values. All the term values are in units of cm^{-1} . Values in parentheses are $G_v(\text{obs}) - G_v(\text{calc})$. Values only calculated and not observed are listed in square brackets.

i	2 ^a	4 ^a	6 ^b	8 ^b	10 ^b	12 ^b
0	1335.0(0.0)	2654.0(-0.3)	3960.0(1.5)	5249.0(0.5)	6522.0(-3.5)	[7790.5]
1	1278.3(0.0)	2598.0(-3.3)	3902.0(-4.9)	[5195.6]	6464.0(-5.3)	7728.0(-1.9)
2		2545.2(-3.2)	3853.0(-5.2)	5141.0(-7.5)	6411.0(-9.3)	[7676.8]
3			3804.0(-5.8)	5097.0(-8.1)	6367.0(-11.0)	[7631.4]
4				[5062.3]	6328.0(-12.9)	[7593.7]
5					[6305.1]	[7563.6]
6						[7537.3]
i	14	16	18	20	22	24
0	9045.0(1.2)	10287.0(1.3)	11516.7(0.6)	12734.7(-0.3)	13942.0(-0.1)	[15137.3]
1	8977.0(-1.5)	10214.7(-0.8)	11440.7(-0.3)	12655.0(0.0)	13857.5(0.2)	[15047.8]
2	[8920.7]	[10153.0]	11373.4(-0.3)	12583.3(0.3)	13782.0(1.2)	[14966.6]
3	[8870.7]	10095.8(-2.3)	11314.9(0.6)	12520.4 (1.3)	13715.5(3.0)	[14894.2]
4	[8828.5]	[10013.0]	11264.1(1.0)	12466.2(2.5)	13657.4(4.3)	[14830.9]
5	[8794.6]	10010.6(-2.3)	11221.4(0.7)	12420.2(2.5)	13607.8(4.2)	[14778.3]
6	[8769.6]	[9984.0]	11187.8(-0.8)	12381.9(-1.0)	13566.5(0.3)	[14738.3]
7	[8755.5]	[9964.5]	11161.2(-2.6)	12355.8(2.9)	13534.9(3.6)	[14698.5]
8		[9937.0]	[11129.0]	12311.5(-0.2)	[13484.2]	[14945.7]
9			[11076.9]	[12255.3]	13426.9(3.9)	[14579.6]
10				[12182.1]	13338.8(-7.6)	14496.6(-2.5)
11					[13253.0]	[14402.5]
12						[14288.9]
i	26	28	30 ^c	32 ^c	34	36 ^c
0	16318.7(-1.6)	17489.3(-1.6)	18648.2(-0.7)	19794.3(0.6)	20928.3 (2.9)	22048.1(4.6)
1	16224.1(-1.9)	17389.6(-2.4)	18542.7(-2.6)	[19685.6]	20811.2(-1.5)	[21926.2]
2	[16140.5]	17299.0(-3.0)	18448.9(-2.0)	[19586.9]	20707.7(-2.1)	[21819.1]
3	16063.9(0.1)	[17221.3]	18366.6(0.3)	[19498.4]	20619.3(1.9)	[21722.9]
4	15998.8(1.9)	17151.6(0.8)	18292.3(0.1)	[19420.9]	20532.6(-4.0)	[21638.9]
5	15943.5(2.2)	17093.3(1.0)	[18231.2]	[19357.4]	20470.9(0.2)	[21570.7]
6	15896.4(-2.3)	17043.9(-3.1)	[18183.0]	[19306.4]	[20416.6]	[21513.5]
7	15858.3(4.3)	[16997.6]	[18128.7]	[19247.2]	[20352.5]	[21444.4]
8	15790.4(-5.5)	[16934.0]	[18059.9]	[19173.0]	[20273.1]	[21359.7]
9	[15724.7]	[16857.7]	[17978.3]	[19086.1]	[20180.7]	[21261.8]
10	[15639.7]	[16768.0]	[17883.7]	[18986.3]	[20075.6]	[21151.2]
11	[15539.5]	[16663.7]	[17774.8]	[18872.7]	[19956.9]	[21027.2]
12	[15422.8]	[16543.4]	[17650.6]	[18744.0]	[19823.5]	[20888.8]
13	[15288.7]	16412.6(6.5)	[17509.7]	[18599.2]	[19674.4]	[20734.9]
14		[16251.1]	[17351.4]	[18437.3]	[19508.4]	[20564.5]
15			17172.4(-2.5)	[18257.3]	[19324.7]	[20376.8]
16				[18058.7]	[19122.6]	[20170.8]
17					[18901.3]	[19945.9]
18						[19701.4]

^aIR data; Ref. 14.^bDF data; Ref. 6.^cSEP data; Ref. 10.

$$\begin{aligned}
& \langle v_1, v_2^l, v_3 | \mathbf{H}^{\text{eff}} | v_1, (v_2 - 2)^l, v_3 + 1 \rangle \\
&= \frac{1}{2\sqrt{2}} \left\{ k_{223} + \lambda_1 \left(v_1 + \frac{1}{2} \right) + \lambda_2 v_2 + \lambda_3 (v_3 + 1) \right\} \\
& \quad \times \sqrt{(v_2^2 - l^2)(v_3 + 1)}, \quad (2)
\end{aligned}$$

where λ_i represents the interaction through the next to lowest term $k_{ii223}q_i^2q_2^2q_3$ in the potential function. The resonance term, $k_{ii223}q_i^2q_2^2q_3$, has the same selection rules as the primary one, $k_{223}q_2^2q_3$, among the quasidegenerate basis states. In the present SEP experiment, only the $l=0$ levels were observed. Moreover, there are no experimental observations yet of highly excited vibrational levels with $v_1 \neq 0$. Thus,

hereafter we will concentrate on polyads with $v_1=0$ and $l=0$. In this analysis, the vibrational term values of 81 levels of $v_1=0$ and $l=0$ were used in the fit. The vibrational term values used in the fit are listed in Table II. Vibrational assignments were carried out as follows. In the case of the lower- P polyads, since the energy regions of each polyad do not overlap with each other, vibrational assignments of the levels observed were readily carried out. First, we performed the least-squares fit using the term values of the lower- P levels. Then, term values for the higher- P polyads were estimated using the molecular constants obtained. Second, we compared between the term values observed and those estimated for the next several higher- P polyads, and made the

TABLE III. The fit parameters and their standard deviation, σ , obtained in the global fit of the bend-CP stretch polyad of HCP. All values are in unit of cm^{-1} . Values in parentheses are statistical error (1σ).

Parameter	Observed ^a	Calculated ^b
ω_2^0	671.360(27)	635.82(13)
ω_3^0	1284.629(35)	1241.63(26)
x_{22}^0	-2.503(10)	1.093(15)
x_{23}^0	-2.953(40)	-6.109(50)
x_{33}^0	-3.814(14)	-4.762(56)
y_{222}^0	-0.02623(31)	-0.11317(38)
y_{223}^0	-0.1132(15)	0.0434(17)
y_{233}^0	-0.1094(30)	0.1303(35)
y_{333}^0	-0.0526(10)	0.0124(30)
$k_{223} + \lambda_1/2$	17.10(15)	15.39(19)
λ_2	-0.484(12)	-0.1070(91)
λ_3	0.2756(86)	0.1442(78)
σ	6.19	3.35

^aFit of all observed vibrational term values.

^bFit of the vibrational term values calculated in the theoretical study (Ref. 11).

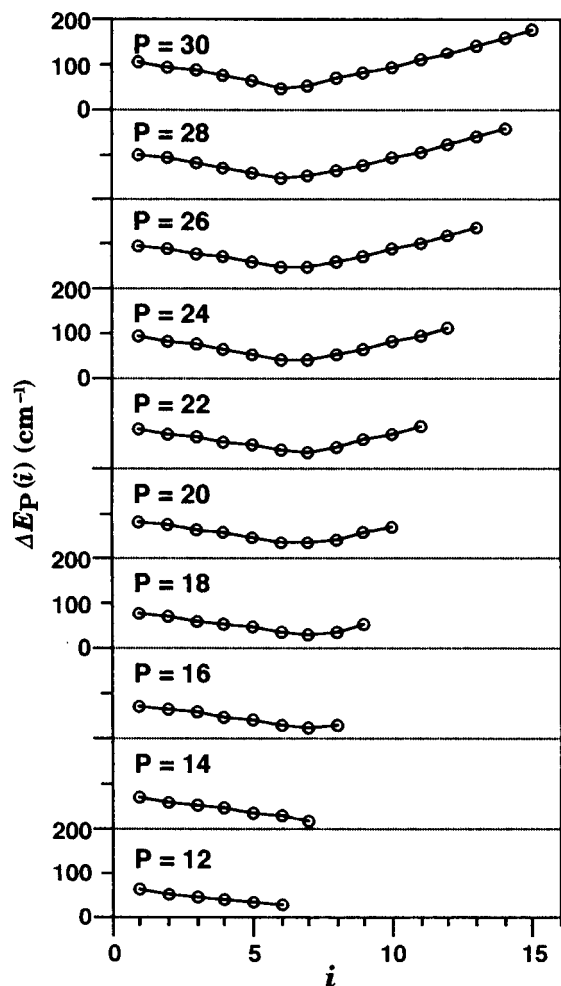


FIG. 4. Plot of the intrapolyad level spacings. The diagnostically significant minimum in the adjacent level spacings first appears in the $P=16$ polyad, and its location matches the onset of “isomerization” levels as identified from both the nodal structure and the mode purity of the eigenvectors.

additional vibrational assignments. Third, we repeated the least squares fit of all previously and newly assigned vibrational levels. We repeated the above iterative procedure for vibrational level assignments. Several levels observed in this study could not be assigned as members of a bend-CP stretch polyad with $v_1=0$. They might eventually be assignable as levels with $v_1 \neq 0$ or levels with $v_1=0$ which are accidentally perturbed by the levels with $v_1 \neq 0$. In addition to the vibrational term values observed in this study, all term values observed in the IR absorption,¹⁴ DF,⁶ and previous SEP (Refs. 10 and 13) studies were included. Appropriate uncertainties for each measurement were taken into account in the least-squares fit. Fit parameters obtained are listed in Table III. The calculated vibrational energies are also listed in Table II. The agreement between the observed and calculated vibrational energies is satisfactory.

C. Intrapolyad level spacings

Kellman and co-workers analyzed the classical phase space structures of bend-stretch (Fermi) resonance systems and showed that a “dip” or minimum in the intrapolyad level spacings corresponds to a qualitative change in the character of the vibrational levels.¹⁷ In Fig. 4, the intrapolyad level spacings of HCP $\tilde{X}^1\Sigma^+$ were plotted, where the calculated vibrational term values were used. It is clearly seen that a minimum in the intrapolyad level spacings first appears above $P=16$ in our analysis. Based on Kellman’s interpretation, the existence of a minimum in the intrapolyad level spacings is evidence for the existence of two distinct families of bending states: the “normal-mode-type” and the “isomerization” states. Moreover, we consider this feature to be direct evidence for the generation of the “isomerization” levels by the bend-CP polyad model. In their theoretical study, Schinke and co-workers have also found similar minima in the intrapolyad level spacings.¹¹

D. Eigenvector analysis of the bend-CP stretch polyads

Since our treatment is entirely based on traditional spectroscopic procedures, where a diagonalization of the zero-order Hamiltonian matrix is carried out for each value of P , the global fit provides us with eigenvectors as well as eigenvalues. In order to extract information about a qualitative change in the character of the vibrational levels, we examined the eigenvectors as described below. The wave function of an eigenstate can be expressed as a linear combination of zero-order basis functions; $|0, v_2, v_3\rangle$. Here, within each polyad, the zero-order basis state $|0, v_2=P, 0\rangle$ corresponds to a pure bend excitation level, while $|0, 0, v_3=P/2\rangle$ is a pure CP stretch overtone level. As mentioned above, intrapolyad interactions are ignored in our treatment, thus the wave function of the i th eigenstate in each polyad, Ψ_i^P , can be expressed as

$$\Psi_i^P = \sum_n a_n^i |0, P-2n, n\rangle. \quad (3)$$

Since the zero-order wave functions are strongly mixed due to the bend-CP stretch resonance, the bend and CP-stretch

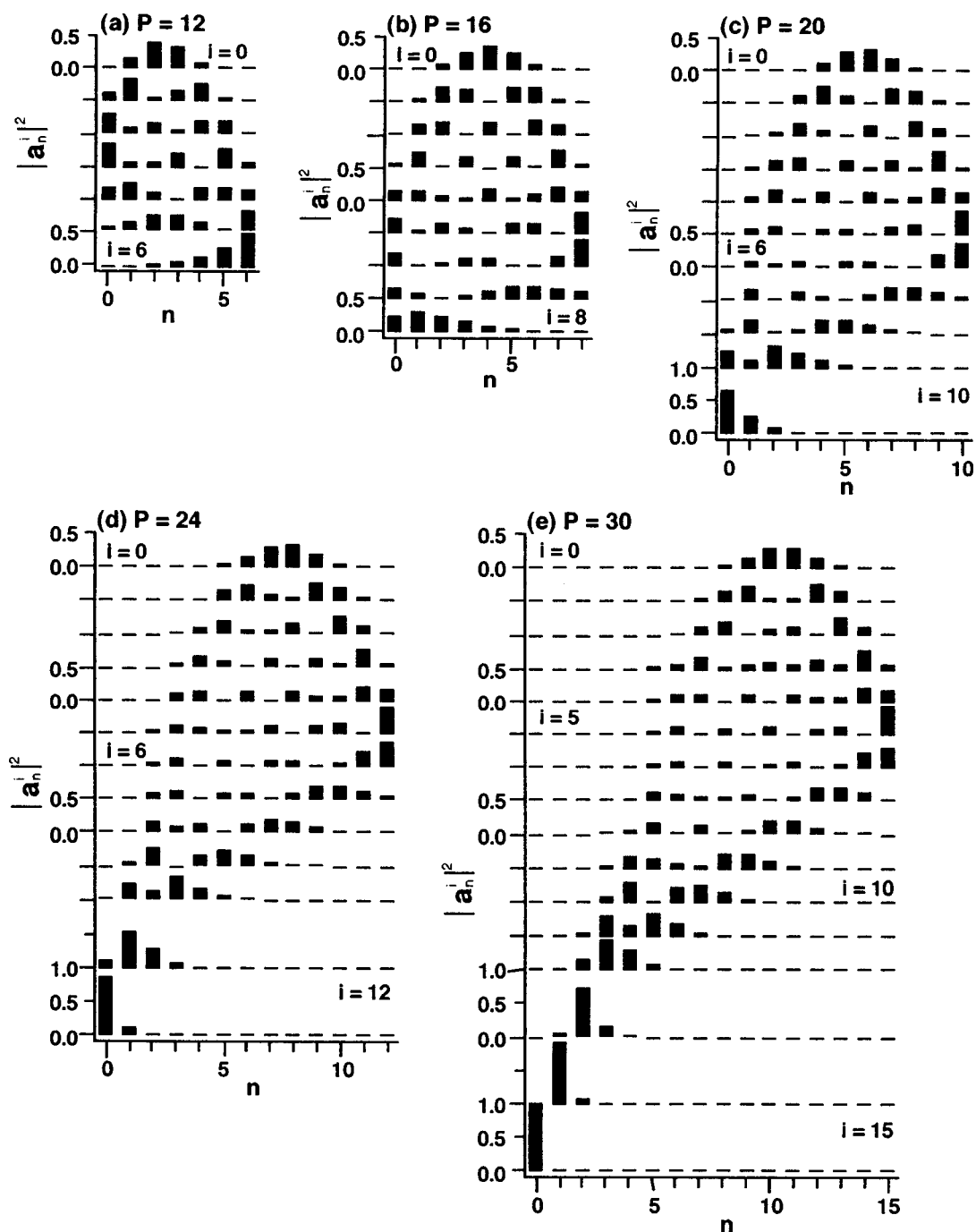


FIG. 5. Plot of the squared eigenvector components for several polyads, based on fits of the observed vibrational energies: (a) $P=12$, (b) $P=16$, (c) $P=20$, (d) $P=24$, and (e) $P=30$. See text for details.

quantum numbers are not useful to specify a vibrational level, while the polyad quantum number, P , is still a good quantum number. Therefore, hereafter, we will refer to the vibrational levels by P and i , where i indicates just the energy rank in each polyad.

The parameters in the \mathbf{H}^{eff} obtained by the global fit of the bend-CP stretch polyad provide all the components of the eigenvector, a_n^i . An eigenvector component squared, $|a_n^i|^2$, corresponds to the weight of the n th zero-order wave function in the i th eigenstate. Figure 5 exhibits the results of the eigenvector analysis of the bend-CP polyad. In general, it is

expected that zero-order wave functions in the polyad are mixed with each other in a complicated manner for each eigenstate in the high energy region. This is certainly true even for the lower- P polyads [see Figs. 5(a) and 5(b)], in which there is no zero-order basis state having a weight of more than 0.5 for any eigenstate. As P increases, the trend of the mixing of the zero-order wave functions changes drastically near $P=20$. The mixing patterns for the top members of each polyad, from $i=0$ to 10 or so, do not change so much and are similar to each other. On the other hand, the bottom member of the $P=20$ polyad is composed

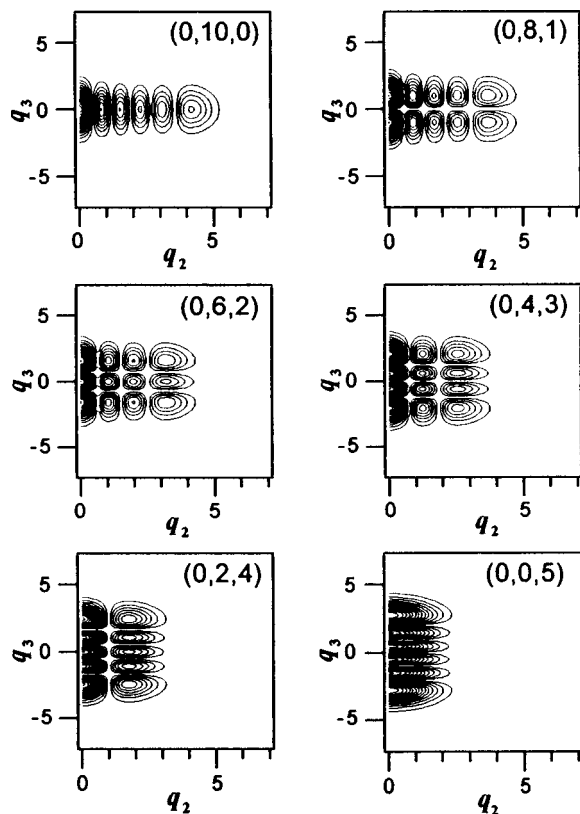


FIG. 6. Plot of the calculated wave functions of the zero-order basis states for the $P=10$ polyad.

of only three zero-order basis states. And in this case, the weight of the pure bend overtone level, $|0,20,0\rangle$, becomes larger than 0.5. As P increases, the bottom member of each polyad more closely approaches being a pure bend overtone level, $|0,P,0\rangle$. In the case of the $P=30$ polyad, the bottom member of this polyad becomes an almost pure bend overtone level (97%). Moreover, the next-to-bottom level also is very close to a pure zero-order state. The form of the wave function of the “isomerization” levels are shown to be very similar to those of the pure bend overtone levels of DCP, where the bend-CP stretch interaction is shown to be very weak, in the theoretical study by Schinke and co-workers.¹¹

An inspection of the wave functions provides us with a clear description of the qualitative change of the vibrational character as mentioned above. Thus, we calculated $2D(q_2, q_3)$ wave functions of the members of the bend-CP stretch polyad, where q_2 and q_3 represent the normal coordinates for the bend and the CP-stretch modes, respectively. In general, it is difficult to draw pictures of wave functions in terms of internal coordinates, such as bond length or bending angle, from experimental observations. In the case of HCP, however, the transformation matrices for the diagonalization of the zero-order basis are known as a result of the global fit of the bend-CP stretch polyad. Therefore, if we knew the wave functions of the zero-order basis, we could obtain those of the eigenstates. Strictly speaking, our zero-order basis states are not the Harmonic oscillator basis, because the diagonal energies contain some anharmonic terms. However, a crude assumption was made here that the wave functions of

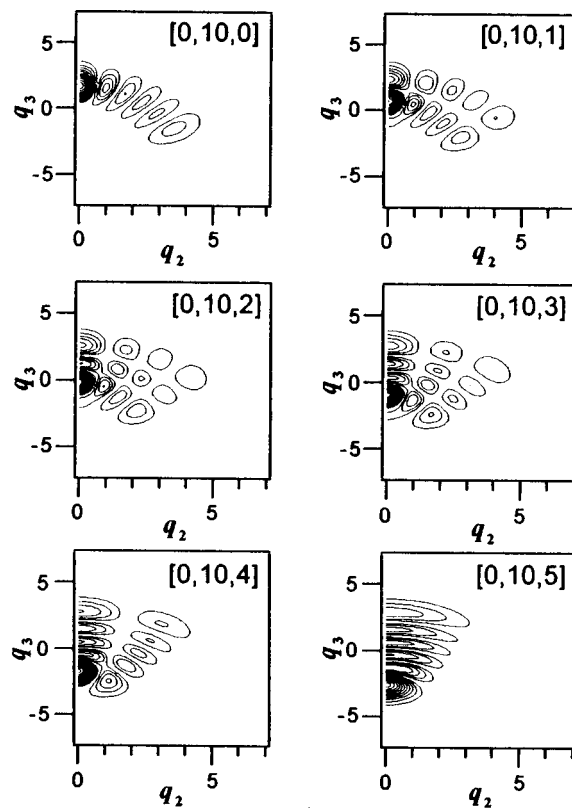


FIG. 7. Plot of the calculated wave functions of the eigenstates of the $P=10$ polyad.

the zero-order basis are not significantly distorted from those of the Harmonic oscillator basis. A wave function of the zero-order basis, $\Phi_{v_2, v_3}(q_2, q_3)$, is represented as a direct product of wave functions for the degenerate bend, $\phi_{v_2, l}(q_2)$, and CP-stretch modes, $\phi_{v_3}(q_3)$,

$$\Phi_{v_2, v_3}(q_2, q_3) = \phi_{v_2, l}(q_2) \phi_{v_3}(q_3), \quad (4)$$

where

$$\phi_{v_2, l}(q_2) = N_{v_2, |l|} \exp(-q_2^2/2) q_2^{|l|} L_{(v_2+|l|)/2}^{|l|}(q_2^2) \quad (5)$$

and

$$\phi_{v_3}(q_3) = N_{v_3} \exp(-q_3^2/2) H_{v_3}(q_3), \quad (6)$$

respectively. L and H are the associated Laguerre and Hermite polynomials, respectively. In Fig. 6, the wave functions of the zero-order basis states for the $P=10$ polyad are exhibited, whereas those of the eigenstates are shown in Fig. 7. The mixing of the two vibrational modes, the bend and the CP-stretch, is well represented by the picture of the wave function of the $[0,10,0]$ level. Figures 8, 9, and 10 show the wave functions of the members of the $P=14$, 16, and 20 polyads, respectively. The wave functions of the top few members, with $i=0-3$ or 4, exhibit quite similar behaviors within each polyad. The only difference is the number of nodes. In the case of $P=14$, the wave functions are similar to those of the $P=10$ polyad. On the contrary, the wave function for the bottom member of the $P=16$ polyad, which is the $[0,16,8]$ level, suddenly exhibits a qualitatively different structure from the other members of this polyad. The

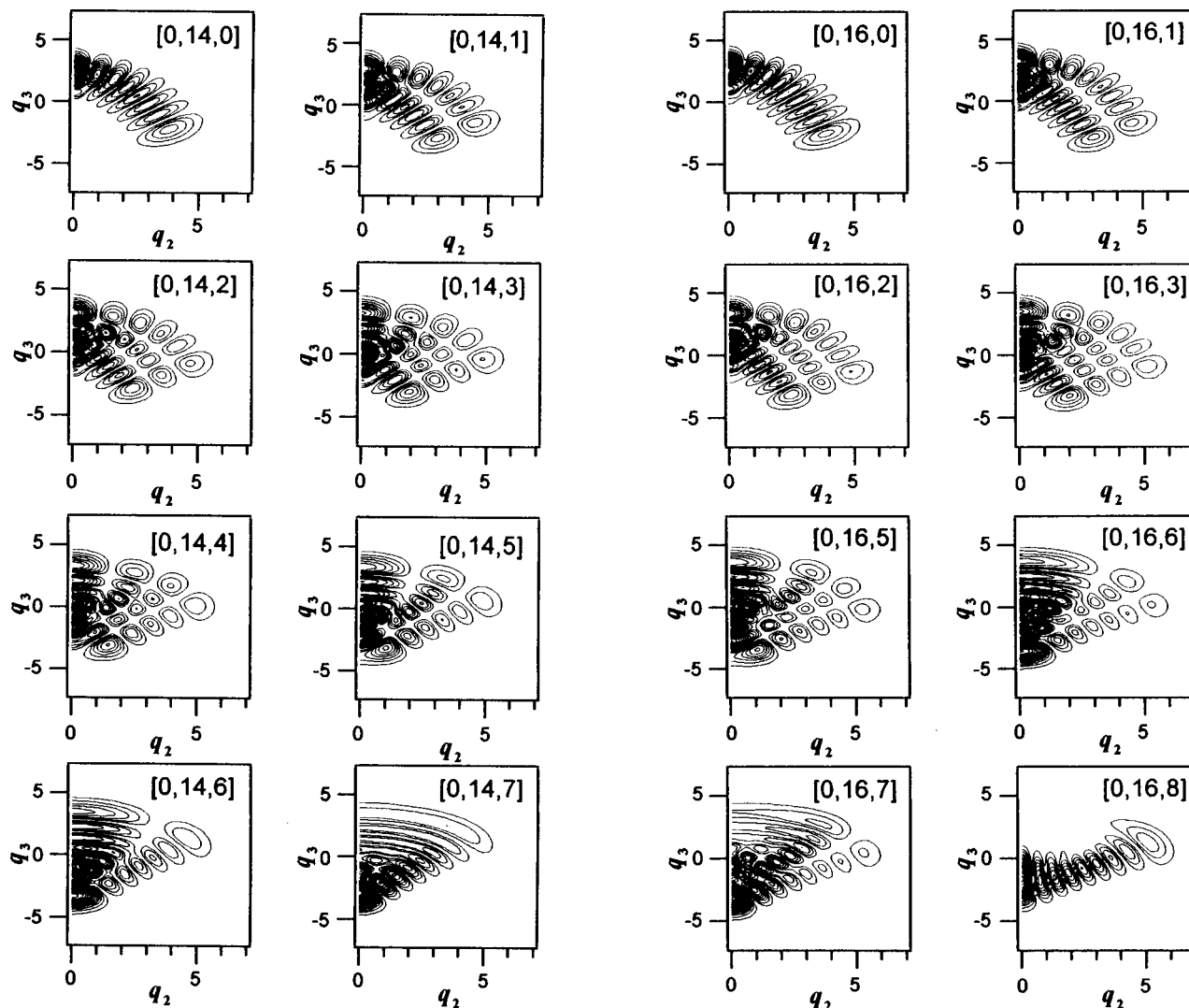


FIG. 8. Plot of the calculated wave functions of the eigenstates of the $P=14$ polyad.

structure of the wave function of this $[0,16,8]$ level is close to that of a pure zero-order pure bend state. Thus, we assigned this $[0,16,8]$ level as the lowest energy “isomerization” level. In the case of the $P=20$ polyad, the bottom three levels have wave functions similar to that of the $[0,16,8]$ level, that is the “isomerization” one. As described in Sec. IV C, the intrapolyad level spacing plot *also* indicated that the lowest energy “isomerization” level is the $[0,16,8]$. Thus, both of these two points of view, the intrapolyad level spacings and inspection of the nodal structure of the wave functions, provide consistent interpretations. Although our calculation of the wave functions is a very naive one, these pictures of the wave functions clearly exhibit the qualitative change of the vibrational structure that is predicted by the theoretical study!¹¹

Finally, in order to further confirm that the qualitative change of the vibrational character found in our eigenvector analysis corresponds to that predicted by the theoretical study, we applied the same eigenvector analysis to the vibrational energies obtained from the Schinke’s theoretical calculation.¹⁸ The same Hamiltonian matrix model was used.

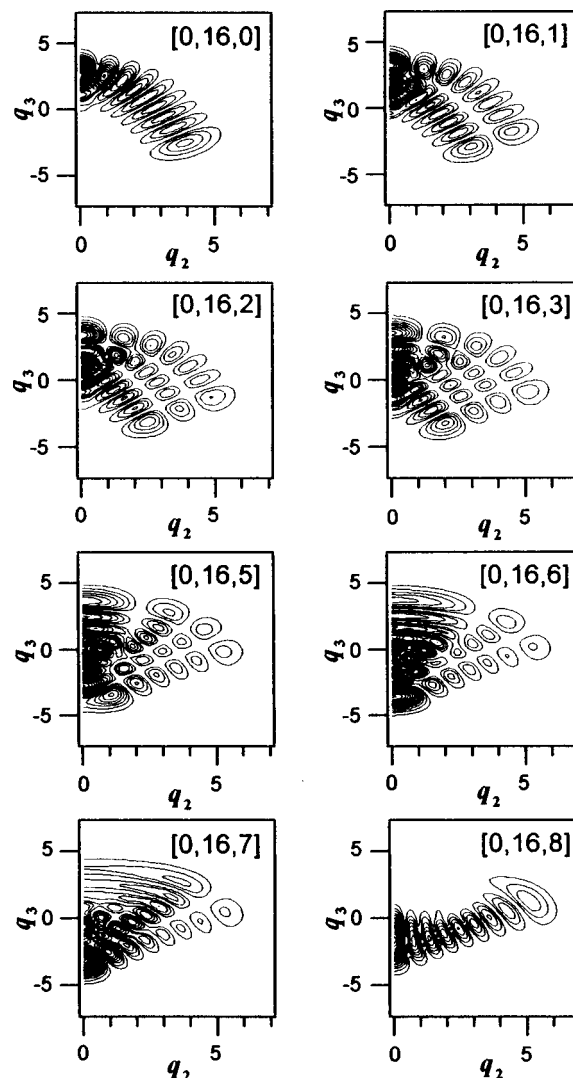


FIG. 9. Plot of the calculated wave functions of the eigenstates of the $P=16$ polyad.

The values of fit parameters obtained are also listed in Table III. All of the vibrational level energies of the polyads with $P=2$ to 30, except for the levels that are predicted to be perturbed by $v_1 \neq 0$ levels, were used in the fit. The fit was satisfactory, and Fig. 11 shows the result. The qualitative change of the mixing patterns in the zero-order basis set is the same as those obtained based on experimental observations. This eigenvector analysis also confirmed that the lowest energy or first “isomerization” level is the bottom one of the $P=26$ polyad. This onset of “isomerization” levels agrees well with Schinke’s theoretical prediction. Thus, the eigenvector analysis shows clearly that the “isomerization” levels are generated from the bend-CP stretch polyad and are definitely not symptomatic of a breakdown of the polyad structure.

E. Interaction with the CH stretch mode

In the case of the $HAB \leftrightarrow ABH$ isomerization, the reaction coordinate must be represented by a combination between the distance of H from the CP center of mass and the bending angle. Therefore, in order to completely describe the

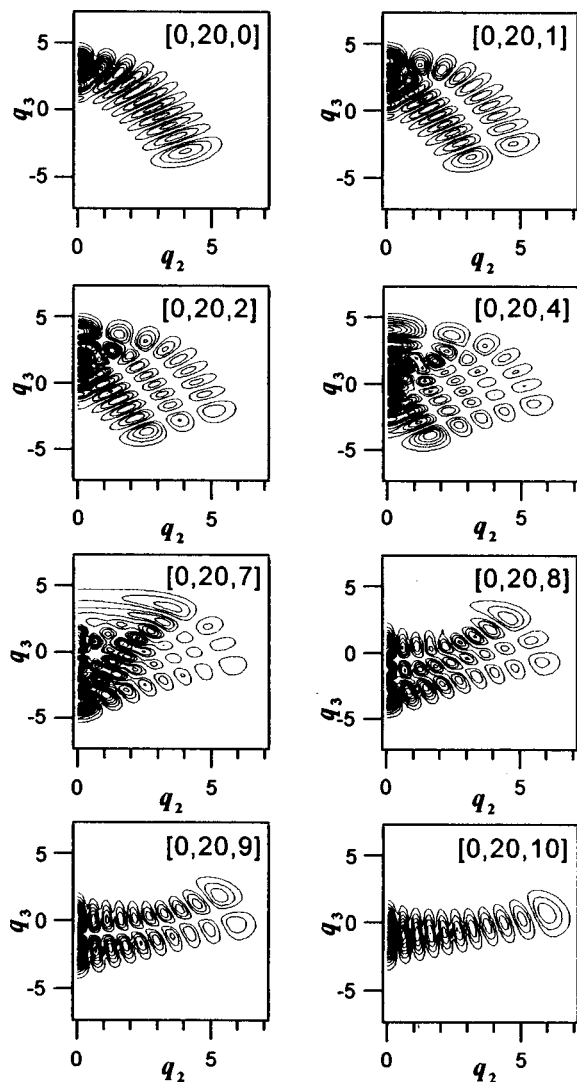


FIG. 10. Plot of the calculated wave functions of the eigenstates of the $P=20$ polyad.

“isomerization” of HCP, it is necessary to include in the \mathbf{H}^{eff} an interaction between the CH stretch and the bending modes. However, as shown in Fig. 12, one can see that the CH bond length does not change significantly along the low energy region of the minimum energy isomerization path. The CH bond length begins to change rapidly when the bond angle decreases to 70° and the energy is about $18\,000\text{ cm}^{-1}$ above the minimum of the potential energy surface. This indicates that the interaction between the CH stretch and bending modes only becomes significant at higher energy than most of our SEP spectra. Thus, although our analysis has not yet taken such an interaction into account, the analysis must be valid at least in the energy region of $E_{\text{VIB}} \leq 15\,000\text{ cm}^{-1}$. In other words, the generation of the “isomerization” states of HCP is exclusively due to the bend-CP stretch polyad. In their PO analysis, Schinke and co-workers reported that there are three saddle-node type bifurcations of the POs. The first bifurcation, [SN1], corresponds to the generation of the “isomerization” states that we have analyzed here. The second bifurcation, [SN2], which emerges at $21\,000\text{ cm}^{-1}$ above the minimum of the

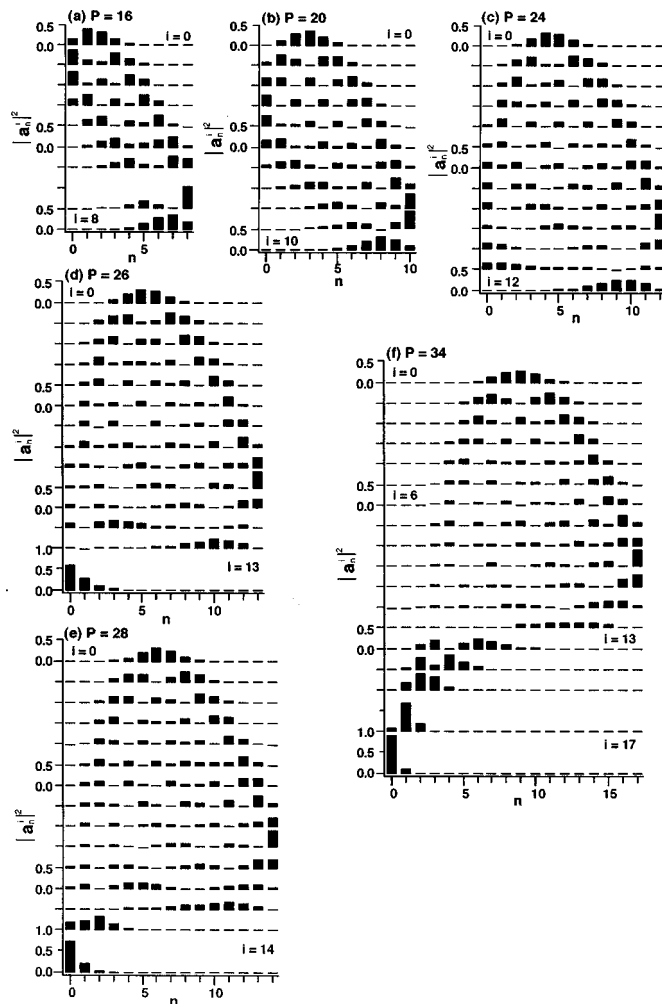


FIG. 11. Plot of the squared eigenvector components for several polyads based on fits of the theoretical vibrational energies: (a) $P=16$, (b) $P=20$, (c) $P=24$, (d) $P=26$, (e) $P=28$, and (f) $P=34$.

potential well, might correspond to the onset of the interaction with CH stretch. In order to investigate the onset of interaction with CH stretch, new experiments on highly excited vibrational levels with $v_1 \neq 0$ are being performed.

F. Comparison with the previous SEP study

In a previous analysis of the results of SEP spectra,¹⁰ we performed a partial analysis of the bend-CP stretch polyad in the high energy region. At that time, there was an inconsistency between our analysis and Winnemisser’s analysis.¹⁴ This inconsistency came from an inappropriate assumption about vibrational assignments within each polyad. In the former DF (Ref. 6) and SEP (Refs. 9 and 10) spectra, the highest energy level in each polyad was assigned to be $(0,P,0)$, the next level is $(0,P-2,1)$, and so on. These assignments were based on the observation of a very smooth vibrational level spacing, $\Delta G_2(v_2) = G(0,v_2+1,0) - G(0,v_2-1,0)$ (see Fig. 11 in Ref. 10). In contrast, the highest energy level in the high- P polyad is predicted *not* to be the pure bend overtone level, $(0,P,0)$, using the molecular constants obtained by Winnemisser and co-workers.¹⁴ In the present study, however,

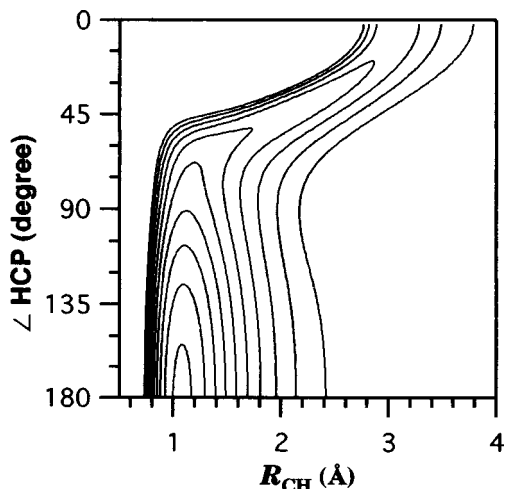


FIG. 12. 2D potential surface of HCP. The CP bond distance was fixed to 1.588 Å. The computer program cited as Ref. 10 in Ref. 8 was used in plotting this figure.

our new analysis of the bend-CP stretch polyad removed this inconsistency and revealed that the highest energy levels in polyad are not the $(0, P, 0)$ levels. The smooth change in the vibrational level spacing, which led us to this inappropriate assignment, may come from the fact that all of the highest energy levels in the polyad have quite similar wave functions. In their analysis of the Fermi interaction of HCP, Winnewisser and co-workers treated the off-diagonal matrix element for the Fermi interaction as

$$\langle v_1, v_2^l, v_3 | \mathbf{H}^{\text{eff}} | v_1, (v_2 - 2)^l, v_3 + 1 \rangle = \frac{k_{223}}{2\sqrt{2}} \sqrt{(v_2^2 - l^2)(v_3 + 1)}. \quad (7)$$

They obtained slightly different values of k_{223} , 16.8782 and 16.345 cm^{-1} , from deperturbations for the $(0, 2^0, 0) - (0, 0^0, 1)$ and the $(0, 3^1, 0) - (0, 1^1, 1)$ pairs, respectively. Winnewisser's k_{223} corresponds to our $k_{223} + \lambda_1(v_1 + \frac{1}{2}) + \lambda_2 v_2 + \lambda_3(v_3 + 1)$. Although our global fit of the bend-CP stretch polyad did not include the $l \neq 0$ levels, the values corresponding to Winnewisser's k_{223} for the $(0, 2^0, 0) - (0, 0^0, 1)$ and the $(0, 3^1, 0) - (0, 1^1, 1)$ pairs are well reproduced to be 16.407 and 15.923 cm^{-1} , respectively. Thus, this supports the validity of our global fit of the bend-CP stretch polyad.

V. CONCLUSION

We have carried out a global fit of the bend-CP stretch polyad of HCP using a traditional spectroscopic effective Hamiltonian matrix model. The intrapolyad level spacings and the eigenvector analysis indicate that a qualitatively new

class of "isomerization" levels is generated directly by the bend-CP stretch polyad structure. Moreover, the eigenvector analysis reveals the change in the character of the vibrational levels, as the polyad quantum number increases. Although this eigenvector analysis is a traditional method, it can be a powerful tool in investigating strongly coupled systems at high excitation energy. This is a very clear demonstration that one can extract information about the change in the character of the vibrational modes directly from the *experimentally* observed spectra.

ACKNOWLEDGMENTS

The authors are very grateful to Professor R. Schinke for providing a copy of Ref. 11 prior to publication and also the results of the vibrational level energy calculation. R.W.F. thanks the AFOSR for continuing support of this research (Grant No. F49620-97-1-0040).

¹Molecular Dynamics and Spectroscopy by Stimulated Emission Pumping, edited by H.-L. Dai and R. W. Field (World Scientific, Singapore, 1995).

²S. C. Farantos, *Int. Rev. Phys. Chem.* **15**, 345 (1996).

³For reviews, see M. E. Kellman, *Molecular Dynamics and Spectroscopy by Stimulated Emission Pumping*, edited by H.-L. Dai and R. W. Field (World Scientific, Singapore, 1995), Chap. 25; M. E. Kellman, *Annu. Rev. Phys. Chem.* **46**, 395 (1995).

⁴For recent examples, see H.-J. Werner, C. Bauer, P. Rosmus, H.-M. Keller, M. Stumpf, and R. Schinke, *J. Chem. Phys.* **102**, 3593 (1995); H.-M. Keller, H. Floethmann, A. J. Dobbyn, R. Schinke, H.-J. Werner, C. Bauer, and P. Rosmus, *ibid.* **105**, 4983 (1996); H.-M. Keller, M. Stumpf, T. Schröder, C. Stöck, F. Temps, R. Schinke, H.-J. Werner, C. Bauer, and P. Rosmus, *ibid.* **106**, 5359 (1997).

⁵J. M. Bowman, B. Gazdy, J. A. Bentley, T. J. Lee, and C. E. Dateo, *J. Chem. Phys.* **99**, 308 (1993).

⁶K. K. Lehmann, S. C. Ross, and L. L. Lohr, *J. Chem. Phys.* **82**, 4460 (1985).

⁷N. L. Ma, S. S. Wong, M. N. Paddon-Row, and W.-K. Li, *Chem. Phys. Lett.* **213**, 189 (1993).

⁸S. C. Farantos, H.-M. Keller, R. Schinke, K. Yamashita, and K. Morokuma, *J. Chem. Phys.* **104**, 10055 (1996).

⁹Y.-T. Chen, D. M. Watt, R. W. Field, and K. K. Lehmann, *J. Chem. Phys.* **93**, 2149 (1990).

¹⁰H. Ishikawa, Y.-T. Chen, Y. Ohshima, J. Wang, and R. W. Field, *J. Chem. Phys.* **105**, 7383 (1996).

¹¹C. Beck, H.-M. Keller, S. Y. Grebenshchikov, R. Schinke, S. C. Farantos, K. Yamashita, and K. Morokuma, *J. Chem. Phys.* **107**, 9818 (1997).

¹²Since the generation of "isomerization" states corresponds to a saddle node bifurcation of the bending periodic orbit diagram, Schinke and co-workers refer to them as SN states in their paper.

¹³H. Ishikawa, C. Nagao, N. Mikami, and R. W. Field, *J. Chem. Phys.* **106**, 2980 (1997).

¹⁴M. Jung, B. P. Winnewisser, and M. Winnewisser (submitted).

¹⁵S. A. B. Solina, J. P. O'Brien, R. W. Field, and W. F. Polik, *Ber. Bunsenges. Phys. Chem.* **99**, 555 (1995); S. A. B. Solina, J. P. O'Brien, R. W. Field, and W. F. Polik, *J. Phys. Chem.* **100**, 7797 (1996).

¹⁶P. F. Bernath, M. Dulick, and R. W. Field, *J. Mol. Spectrosc.* **86**, 275 (1981).

¹⁷J. Svitak, Z. Li, J. Rose, and M. E. Kellman, *J. Chem. Phys.* **102**, 4340 (1995).

¹⁸R. Schinke (private communication).